11-16-2009

Phaseless Three-Dimensional Optical Nanoimaging

Alexander A. Govyadinov
University of Pennsylvania, algov@seas.upenn.edu

George Y. Panasyuk
University of Pennsylvania, georgey@seas.upenn.edu

John C. Schotland
University of Pennsylvania, schotland@seas.upenn.edu

Suggested Citation:
Govyadinov, A.A., G.Y. Panasyuk and J.C. Schotland. (2009). "Phaseless Three-Dimensional Optical Nanoimaging." *Physical Review Letters.* 103, 213901.

http://dx.doi.org/10.1103/PhysRevLett.103.213901

Phaseless Three-Dimensional Optical Nanoimaging

Abstract
We propose a method for optical nanoimaging in which the structure of a three-dimensional inhomogeneous medium may be recovered from far-field power measurements. Neither phase control of the illuminating field nor phase measurements of the scattered field are necessary. The method is based on the solution to the inverse scattering problem for a system consisting of a weakly-scattering dielectric sample and a strongly-scattering nanoparticle tip. Numerical simulations are used to illustrate the results.

http://dx.doi.org/10.1103/PhysRevLett.103.213901

Phaseless Three-Dimensional Optical Nanoimaging

Alexander A. Govyadinov,* George Y. Panasyuk,† and John C. Schotland‡

Department of Bioengineering, University of Pennsylvania, Philadelphia, Pennsylvania, USA

(Received 20 June 2009; revised manuscript received 8 October 2009; published 16 November 2009)

We propose a method for optical nanoimaging in which the structure of a three-dimensional inhomogeneous medium may be recovered from far-field power measurements. Neither phase control of the illuminating field nor phase measurements of the scattered field are necessary. The method is based on the solution to the inverse scattering problem for a system consisting of a weakly-scattering dielectric sample and a strongly-scattering nanoparticle tip. Numerical simulations are used to illustrate the results.

DOI: 10.1103/PhysRevLett.103.213901 PACS numbers: 42.30.Wb, 42.25.Fx

The development of tools for three-dimensional imaging of nanostructures is of considerable current interest [1–4]. There are multiple potential applications including inspection of semiconductor devices, detection of atoms buried beneath surfaces and characterization of biologically important supramolecular assemblies, among others. Optical methods, especially near-field scanning optical microscopy (NSOM) and its variants, hold great promise for nanoscale imaging due to their subwavelength resolution, spectroscopic sensitivity to chemical composition, and nondestructive nature. Although traditionally viewed as a technique for imaging surfaces, near-field microscopy has recently demonstrated the capacity to detect subsurface structure [1,3]. Experiments in which a near-field probe is scanned over a three-dimensional volume outside the sample suggest that information on the three-dimensional structure of the sample is encoded in the data. That is, the measured intensity viewed as a function of height above the sample is seen to depend upon the depth of subsurface features. However, the intensity images obtained in this manner are not tomographic, nor are they quantitatively related to the optical properties of the medium.

The above noted difficulties have led to the use of inverse-scattering theory to elucidate the precise manner in which three-dimensional subwavelength structure is encoded in the optical near field [5–13]. Results in this direction have been reported for two-dimensional reconstructions of thin samples [8] and also for three-dimensional inhomogeneous media [14]. In either case, solution of the inverse scattering problem generally requires measurements of the optical phase, in the form of a near-field hologram, an experiment that is notorious for its difficulty. The replacement of phase measurements by phase control of the illuminating field has also been proposed [7]. In this approach, the power extinguished from an incident evanescent wave field is used to reconstruct the imaginary (absorptive) part of the dielectric susceptibility, leaving the real part unrecoverable.

In this Letter we propose a method for nanoscale optical tomography that relies neither on phase measurements of the scattered field nor on phase control of the illuminating field. Our approach enables the reconstruction of the *complex-valued* dielectric susceptibility with subwavelength resolution in three dimensions. As a proxy for the optical phase, we introduce a controlled scatterer, such as an atomic force microscopy tip, into the near field of the sample. The power extinguished from the incident field, which illuminates the sample and the tip, is then measured. Since the tip is placed externally to the sample, changing its position controls the pattern of illumination, which thus modifies the power extinguished from the incident beam. The crucial difference from conventional holographic techniques is that the interference pattern is regulated by an *internal* degree of freedom of the system (regarded as the sample plus the tip) rather than by external illumination. The burden of phase-resolved measurements or phase-controlled illumination is thus replaced by the problem of controlling the position of the tip. The readily available nanometer precision in probe positioning that is achievable in atomic force microscopy, in combination with the simplicity of far-field measurements of the extinguished power, is expected to allow the practical realization of the proposed method.

We begin by considering an experiment in which a sample is deposited on a planar substrate. The lower half-space $z < 0$ (the substrate) is taken to have a constant index of refraction n. The sample occupies the upper half-space $z \geq 0$ and is assumed to be nonmagnetic. The index of refraction in the upper half-space varies within the sample, but otherwise has a value of unity. The upper half-space also contains the tip which is placed in the near field of the sample. The sample and tip are illuminated from below by a monochromatic evanescent plane wave and the power extinguished from the illuminating field is monitored, as shown in Fig. 1.

The electric field $\mathbf{E}$ in the upper half-space obeys the reduced wave equation

$$\boldsymbol{\nabla} \times \boldsymbol{\nabla} \times \mathbf{E}(\mathbf{r}) - k_0^2 \mathbf{E}(\mathbf{r}) = 4\pi k_0^2 [\eta(\mathbf{r}) + \chi(\mathbf{r})] \mathbf{E}(\mathbf{r}), \tag{1}$$

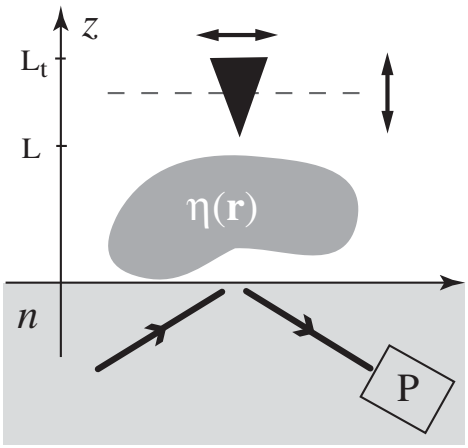

FIG. 1. Illustrating the experiment. The tip scatters the incident evanescent field and modifies the interference pattern in the sample, which has dielectric susceptibility $\eta(\mathbf{r})$. The power P extinguished from the illuminating field is measured as the tip is scanned on a three-dimensional grid in the near zone of the sample.

where η is the generally-complex dielectric susceptibility of the sample, χ is the susceptibility of the tip, $k_0 = 2\pi/\lambda$ is the free-space wave number and the field obeys the necessary interface and boundary conditions. The field is taken to consist of two parts, $\mathbf{E} = \mathbf{E}_i + \mathbf{E}_s$, where $\mathbf{E}_i$ is the incident field and $\mathbf{E}_s$ is the scattered field. The incident field obeys Eq. (1) in the absence of the sample and the tip. The scattered field obeys the integral equation

$$\mathbf{E}_s(\mathbf{r}) = k_0^2 \int \bar{\mathbf{G}}(\mathbf{r}, \mathbf{r}') \cdot \mathbf{E}(\mathbf{r}')[\eta(\mathbf{r}') + \chi(\mathbf{r}')]d^3r', \quad (2)$$

where $\bar{\mathbf{G}}$ is the half-space Green's tensor. The power P_e extinguished from the illuminating field can be obtained using the generalized optical theorem [15]:

$$P_e = \frac{k_0 c}{2} \mathrm{Im} \int_V \mathbf{E}_i^*(\mathbf{r}) \cdot \mathbf{E}(\mathbf{r})[\eta(\mathbf{r}) + \chi(\mathbf{r})]d^3r, \quad (3)$$

where the integration is performed over the volume V, which contains both the sample and the tip.

Suppose that the tip is a strongly-scattering, possibly metallic, nanoparticle and the sample is a weakly-scattering dielectric. We may then compute the electric field perturbatively, accounting for all orders of scattering from the tip and one order of scattering from the sample. We find that the resulting perturbation series can be resummed and, neglecting contributions arising solely from the sample or the tip, consists of a sum of three terms [13]. The first, or "TS", term corresponds to scattering from the tip and then from the sample. The second, or "ST", term is due to scattering from the sample and then from the tip. The third, or "TST" term, arises from scattering first from the tip, then from the sample and finally from the tip. Note that two additional terms originating solely from scattering by the sample or the tip contain no structural information and will be omitted. In practice they can be removed by calibration. To proceed further, we must specify a model for the tip. We treat the tip as a small scatterer with susceptibility $\chi(\mathbf{r}) = \alpha_0 \delta(\mathbf{r} - \mathbf{r}_t)$, where $\mathbf{r}_t$ is the tip's position and α_0 is its polarizability. Resummation of the perturbation series, as explained above, leads to a renormalization of the polarizability of the tip of the form $\alpha = \alpha_0/(1 - 2ik^3\alpha_0/3)$. We note that this result includes radiative corrections to the Lorent-Lorenz form of the polarizability but neglects the dependence on the tip height above the interface [13,16].

It follows from Eq. (3) that the extinguished power can be expressed as a sum of contributions of ST, TS and TST types:

$$P_e(\mathbf{r}_t) = \frac{ck_0^3}{4i} \int \sum_{p=1}^{2} K^{(p)}(\mathbf{r}_t, \mathbf{r}) \eta^{(p)}(\mathbf{r}) d^3r, \quad (4)$$

where $\eta^{(1)}(\mathbf{r}) = \eta^{(2)*}(\mathbf{r}) = \eta(\mathbf{r})$, the kernels $K^{(p)}(\mathbf{r}_t, \mathbf{r})$ are defined by

$$\begin{aligned} K^{(1)}(\mathbf{r}_t, \mathbf{r}) &= -K^{(2)*}(\mathbf{r}_t, \mathbf{r}) \\ &= \alpha \mathbf{E}_i^*(\mathbf{r}_t) \cdot \bar{\mathbf{G}}(\mathbf{r}_t, \mathbf{r}) \cdot \mathbf{E}_i(\mathbf{r}) \\ &\quad + \alpha \mathbf{E}_i^*(\mathbf{r}) \cdot \bar{\mathbf{G}}(\mathbf{r}, \mathbf{r}_t) \cdot \mathbf{E}_i(\mathbf{r}_t) \\ &\quad + \alpha^2 k^2 \mathbf{E}_i^*(\mathbf{r}_t) \cdot (\bar{\mathbf{G}}(\mathbf{r}_t, \mathbf{r}) \bar{\mathbf{G}}(\mathbf{r}, \mathbf{r}_t)) \cdot \mathbf{E}_i(\mathbf{r}_t) \end{aligned} \quad (5)$$

and the dependence of the extinguished power on the tip position has been made explicit.

We will assume that the sample occupies the region $0 \leq z \leq L$ and that it is illuminated by a plane wave of the form $\mathbf{E}_i(\mathbf{r}) = \mathbf{E}_0 \exp(i\mathbf{q}_i \cdot \boldsymbol{\rho} + k_z z)$. Here $\mathbf{r} = (\boldsymbol{\rho}, z)$ and the field has amplitude $\mathbf{E}_0$, transverse wave vector $\mathbf{q}_i$, and $k_z = \sqrt{(nk_0)^2 - q_i^2}$. The extinguished power is measured for a discrete set of tip positions located on a three-dimensional Cartesian grid with transverse spacing h and longitudinal spacing Δz. Note that the tip occupies the region $L < z \leq L_t$ and thus does not overlap the sample.

It will prove useful to perform a two-dimensional lattice Fourier transform of the sampled extinguished power in the plane $z = z_t$, namely $\tilde{P}_e(\mathbf{q}, z_t) = \sum_{\boldsymbol{\rho}} \exp(i\mathbf{q} \cdot \boldsymbol{\rho}) P_e(\boldsymbol{\rho}, z_t)$. Here the sum is carried out over all lattice vectors and $\mathbf{q}$ is restricted to the first Brillouin zone (FBZ) of the lattice. Next, we require the plane-wave decomposition of the tensor Green's function

$$\bar{\mathbf{G}}(\mathbf{r}, \mathbf{r}') = \int \frac{d^2q}{(2\pi)^2} \exp[i\mathbf{q} \cdot (\boldsymbol{\rho} - \boldsymbol{\rho}')] \bar{\mathbf{g}}_{\mathbf{q}}(z, z'), \quad (6)$$

where the form of $\bar{\mathbf{g}}_{\mathbf{q}}$ is given in Ref. [17]. Making use of this result and carrying out the lattice Fourier transform, we find that Eq. (4) becomes

$$\tilde{P}_e(\mathbf{q}, z_t) = \int_0^L \sum_{p=1}^{2} \tilde{K}^{(p)}(\mathbf{q}; z_t, z) \tilde{\eta}^{(p)}(\mathbf{q}, z) dz, \quad (7)$$

where $\tilde{K}^{(1)}(\mathbf{q}; z_t, z)$ is defined as

$$\tilde{K}^{(1)}(\mathbf{q}; z_t, z) = \alpha T\Big[\gamma \mathbf{E}_0^* \cdot \bar{\mathbf{g}}_{\mathbf{q}_i-\mathbf{q}}(z_t, z) \cdot \mathbf{E}_0 + \gamma^* \mathbf{E}_0^* \cdot \bar{\mathbf{g}}_{\mathbf{q}_i+\mathbf{q}}(z, z_t) \cdot \mathbf{E}_0 + \alpha k_0^2 \int \frac{d^2q'}{(2\pi)^2} \mathbf{E}_0^* \cdot (\bar{\mathbf{g}}_{\mathbf{q}'}(z_t, z) \times \bar{\mathbf{g}}_{\mathbf{q}+\mathbf{q}'}(z, z_t)) \cdot \mathbf{E}_0\Big] \quad (8)$$

and $\tilde{K}^{(2)}(\mathbf{q}; z_t, z) = \tilde{K}^{(1)*}(-\mathbf{q}; z_t, z)$. Here $T = ck_0^3/(4ih^2)\exp[-2\mathrm{Im}k_z z_t]$, $\gamma = \exp[ik_z(z - z_t)]$ and $\tilde{\eta}(\mathbf{q}, z) = \int d^2\rho \exp(i\mathbf{q} \cdot \boldsymbol{\rho})\eta(\boldsymbol{\rho}, z)$. Note that for fixed $\mathbf{q}$, Eq. (7) defines a one-dimensional integral equation for $\tilde{\eta}^{(p)}(\mathbf{q}, z)$.

The inverse scattering problem we consider consists of recovering $\eta^{(p)}$, for $p = 1, 2$, from measurements of P_e. This corresponds to solving the integral equation Eq. (7). If it is known, *a priori*, that the susceptibility η is purely real or imaginary, then the inverse problem is formally determined and the solution to Eq. (7) is readily obtained by singular value decomposition (SVD) [6,7]. However, if η is complex valued, the inverse problem is underdetermined. To resolve this difficulty, it is necessary to introduce additional data, which we take to consist of a second set of measurements. That is, two sets of measurements must be carried out for each location of the tip, yielding $\tilde{P}_{e1}$ and $\tilde{P}_{e2}$, one for each incident plane wave with transverse wave vectors $\mathbf{q}_{1,2}$ and amplitudes $\mathbf{E}_{1,2}$, respectively. In this manner, it is possible to reconstruct both η and η^* simultaneously, which is equivalent to recovering the real and imaginary parts of η. Following the approach of Ref. [18], we find that the solution to the integral equation (7) is given by the formula

$$\tilde{\eta}^{(p)}(\mathbf{q}, z) = \sum_{z_t, z_t'} \sum_{i,j} \tilde{K}_i^{(p)*}(\mathbf{q}; z_t, z) M_{ij}^{-1}(\mathbf{q}; z_t, z_t') \tilde{P}_{ej}(\mathbf{q}, z_t'),$$

where $i, j = 1, 2$ label the incident waves. Here M_{ij}^{-1} is the inverse of the matrix whose elements are given by

$$M_{ij}(\mathbf{q}; z_t, z_t') = \int_0^L \sum_p \tilde{K}_i^{(p)}(\mathbf{q}; z_t, z) \tilde{K}_j^{(p)*}(\mathbf{q}; z_t', z) dz. \quad (9)$$

An inverse Fourier transform is applied to obtain a transversely bandlimited approximation to $\eta(\mathbf{r})$ with bandwidth $2\pi/h$. Several remarks on this result are necessary. (i) The computation of the inverse of the matrix M is unstable due to the presence of small eigenvalues. We thus regularize M^{-1} according to the formula

$$M^{-1} = \sum_n \frac{1}{\sigma_n^2} \Theta(\sigma_n^2 - \epsilon) |u_n\rangle\langle u_n|, \quad (10)$$

where $|u_n\rangle$ is an eigenvector of M with eigenvalue σ_n^2. The step function Θ serves to cut off eigenvalues that are smaller than ϵ. With the above choice, the solution to the inverse problem is the unique minimum L^2 norm solution of (7). (ii) The inverse problem we have considered is severely ill posed, in the same class as inversion of the Laplace transform [19]. Regularization of M^{-1} restores stability, consistent with the requirement that the resolution in the transverse direction is set by the lattice spacing h and in the longitudinal direction by Δz.

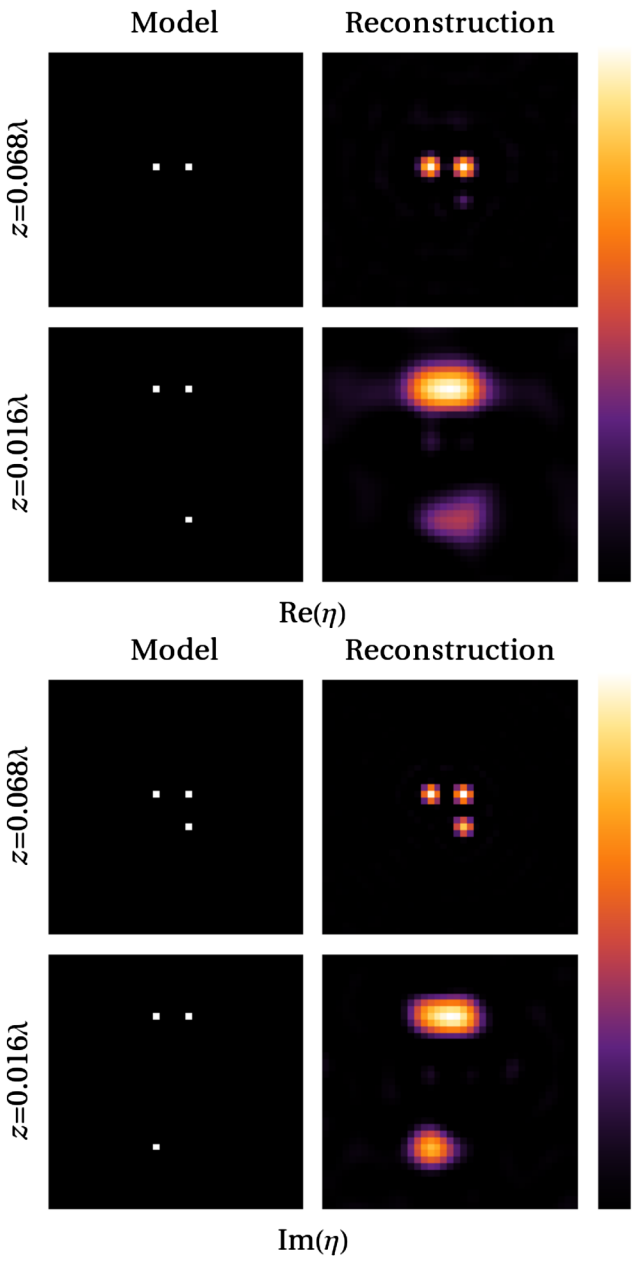

FIG. 2 (color online). The model (left) and simulated reconstructions (right) of $\mathrm{Re}\eta(\mathbf{r})$ and $\mathrm{Im}\eta(\mathbf{r})$. The scatterers are distributed in two planes at $z = 0.016\lambda$ (top) and $z = 0.068\lambda$ (bottom). The scatterers are separated in-plane by 0.05λ and 0.2λ in the x and y directions, respectively. Each image is normalized to its own maximum and any small negative values are not displayed. The field of view of each image is $0.4\lambda \times 0.4\lambda$.

To demonstrate the feasibility of the inversion, we have numerically simulated the reconstruction of $\eta(\mathbf{r})$ for a collection of point scatterers. The left column in Fig. 2 shows the configuration of the scatterers. The tip was modeled as a small sphere of polarizability $\alpha_0 = (\epsilon - 1)/(\epsilon + 2)R^3$ with radius $R = 8 \times 10^{-2}\lambda$ and permittivity $\epsilon = -11.39 + 0.13i$, which corresponds to silver at a wavelength $\lambda = 550$ nm. The incident fields were taken to be evanescent plane waves with transverse wave vectors $\mathbf{q}_1 = (3.15k_0/\pi, 0)$ and $\mathbf{q}_2 = (0, 3.25k_0/\pi)$, and vector amplitudes $\mathbf{E}_1 = (-0.521, -0.714, 0.468)$ and $\mathbf{E}_2 = (0.714, -0.507, 0.483)$, respectively. The susceptibility η was reconstructed on a $40 \times 40 \times 20$ Cartesian grid whose transverse extent was $0.4\lambda \times 0.4\lambda$ and height in the z direction was 0.08λ. The forward data were calculated from Eq. (4) for the positions of the tip center located on the same 40×40 transverse grid with 20 steps of size $\Delta z = 0.001\lambda$ in the z direction, beginning 0.16λ from substrate. The integral in the kernel (8) was numerically evaluated using a trapezoidal rule with 300 points in each direction, spanning six Brillouin zones. The computation of M_{ij}^{-1} was regularized by setting $\epsilon = 10^{-11}$. We note that *a priori* information on the form of the scatter is not employed in the reconstructions. In particular, it is not necessary to assume that the medium is composed of point scatterers.

In Fig. 2 we present reconstructions of the real and imaginary parts of η. Tomographic slices are shown in the planes $z = 0.016\lambda$ and $z = 0.068\lambda$. It can be seen that the scatterers in the top layer (nearest the tip) are better resolved than the scatterers in the deeper layer. This is due to the decay of high-frequency evanescent waves with depth and is a typical feature of tomographic reconstructions in the near field [6]. It may also be observed that the reconstructions of the imaginary part of the susceptibility are of higher quality than those of the real part. This effect may be explained by noting that the extinction of power due to absorption is greater than that due to elastic scattering in the near field, since the optical phase changes minimally in the near-zone of the scatterer.

In conclusion, we have shown that the three-dimensional *subwavelength* structure of an inhomogeneous scattering medium can be recovered from measurements of the extinguished power. Remarkably, neither phase control of the illuminating field nor phase measurements of the scattered field are required. Our approach is based on the solution to the inverse scattering problem for a system consisting of a weakly-scattering sample and a strongly-scattering nanoscale tip. Finally, we note that concepts we have presented are quite general since they can be applied to imaging with any wave field for which the usual apparatus of scattering theory and the optical theorem can be constructed.

The authors are grateful to Professor Vadim A. Markel for valuable discussions. This work was supported by the NSF under the Grant No. DMR0425780 and by the USAFOSR under the Grant No. FA9550-07-1-0096.

*algov@seas.upenn.edu
†georgey@seas.upenn.edu
‡schotland@seas.upenn.edu

[1] T. Taubner, F. Keilmann, and R. Hillenbrand, Opt. Express **13**, 8893 (2005).
[2] N. Anderson, P. Anger, A. Hartschuh, and L. Novotny, Nano Lett. **6**, 744 (2006).
[3] A. Cvitkovic, N. Ocelic, and R. Hillenbrand, Opt. Express **15**, 8550 (2007).
[4] J. Aizpurua, T. Taubner, F. de Abajo, M. Brehm, and R. Hillenbrand, Opt. Express **16**, 1529 (2008).
[5] R. Carminati and J. Greffet, Opt. Commun. **116**, 316 (1995).
[6] P. S. Carney and J. C. Schotland, Appl. Phys. Lett. **77**, 2798 (2000).
[7] P. S. Carney, V. A. Markel, and J. C. Schotland, Phys. Rev. Lett. **86**, 5874 (2001).
[8] P. S. Carney, R. A. Frazin, S. I. Bozhevolnyi, V. S. Volkov, A. Boltasseva, and J. C. Schotland, Phys. Rev. Lett. **92**, 163903 (2004).
[9] P. C. Chaumet, K. Belkebir, and A. Sentenac, Opt. Lett. **29**, 2740 (2004).
[10] K. Belkebir, P. C. Chaumet, and A. Sentenac, J. Opt. Soc. Am. A **22**, 1889 (2005).
[11] A. Sentenac, P. C. Chaumet, and K. Belkebir, Phys. Rev. Lett. **97**, 243901 (2006).
[12] P. Li and G. Bao, Opt. Lett. **32**, 1465 (2007).
[13] J. Sun, P. S. Carney, and J. C. Schotland, J. Appl. Phys. **102**, 103103 (2007).
[14] K. P. Gaikovich, Phys. Rev. Lett. **98**, 183902 (2007).
[15] D. R. Lytle, P. S. Carney, J. C. Schotland, and E. Wolf, Phys. Rev. E **71**, 056610 (2005).
[16] P. de Vries, D. V. van Coevorden, and A. Lagendijk, Rev. Mod. Phys. **70**, 447 (1998).
[17] A. A. Maradudin and D. L. Mills, Phys. Rev. B **11**, 1392 (1975).
[18] V. A. Markel, V. Mital, and J. C. Schotland, J. Opt. Soc. Am. A **20**, 890 (2003).
[19] C. Epstein and J. C. Schotland, SIAM Rev. **50**, 504 (2008).